Ellipsoid Zone Change According to Glaucoma Stage Advancement

AHNUL HA, YOUNG KOOK KIM, JIN WOOK JEOUNG, AND KI HO PARK

• PURPOSE: To compare retinal photoreceptor ellipsoid zone (EZ) intensity between normal eyes and those with different stages of glaucoma.
• DESIGN: Retrospective cross-sectional study.
• METHODS: The study included 37 normal, 38 preperimetric glaucoma, 39 mild-to-moderate glaucoma (visual field [VF] mean deviation [MD]: −7.7 ± 2.0 dB), and 36 severe glaucoma eyes (VF MD: −17.8 ± 3.2 dB). The subjects underwent high-resolution horizontal and vertical line scans through the fovea by spectral-domain optical coherence tomography (SD-OCT). Image processing software was employed to quantify the intensity of the first and second hyperreflective bands corresponding with the external limiting membrane (ELM) and EZ. In order to account for the brightness variation among scans, the relative EZ intensity as the ratio of the second to first reflective band (EZ/ELM) was determined.
• RESULTS: The relative EZ intensity in severe glaucoma eyes was significantly lower than in mild-to-moderate glaucoma eyes (2.46 ± 0.38 vs 3.15 ± 0.43, $P < .001$); also, it was lower in mild-to-moderate than in preperimetric glaucoma eyes (3.15 ± 0.43 vs 3.86 ± 0.44, $P < .001$). However, the comparison between preperimetric glaucoma and normal eyes showed no significant difference (3.86 ± 0.44 vs 4.06 ± 0.40, $P = .751$). In 75 glaucomatous eyes with VF defect, there was a significant correlation between relative EZ intensity and VF MD ($r = 0.83$ and $P < .001$).
• CONCLUSIONS: According to SD-OCT, relative EZ intensity reduction occurs in the mild-to-moderate and severe glaucoma stages. These findings suggest, at least provisionally, that in the course of glaucoma progression, mitochondrial changes in the inner segments of photoreceptors occur. Further investigation is warranted to evaluate the potential clinical significance of EZ intensity reduction in glaucoma. (Am J Ophthalmol 2018;192:1–9. © 2018 The Author(s). Published by Elsevier Inc. This is an open access article under the CC BY-NC-ND license (http://creativecommons.org/licenses/by-nc-nd/4.0/).)

AJO.com Supplemental Material available at AJO.com.
Accepted for publication Apr 28, 2018.

From the Department of Medicine, Seoul National University College of Medicine, Seoul, South Korea; and Department of Ophthalmology, Seoul National University Hospital, Seoul, South Korea.
Inquiries to Ki Ho Park, Department of Ophthalmology, Seoul National University Hospital, Seoul National University College of Medicine, 101 Daehak-ro, Chongno-gu, Seoul 110-744, Republic of Korea; e-mail: kihopark@snu.ac.kr

GLAUCOMA MANIFESTS AS PATHOLOGIC CHANGES in the inner retina's retinal ganglion cells (RGCs).[1,2] It has been observed that degenerative changes in the lateral geniculate nucleus and visual cortex can co-present in glaucomatous eyes by trans-synaptic degeneration and that they occur in relation to the severity of RGCs cell loss.[3] The mechanisms underlying the processes are not yet exactly known, but based on the fact that retinal neuronal cells are closely related both structurally and functionally, it has been posited that outer retinal layer changes might occur as well, according to similar principles. In fact, impaired outer retinal neuronal function as well as cell number reduction in the photoreceptor layer have been demonstrated in glaucomatous eyes.[4–7] Other studies, however, indicate that the histologic evidence for glaucomatous outer retinal layer degenerative changes is lacking.[8,9] In summary, the issue as to whether glaucoma affects the outer retinal layers remains controversial.

Imaging equipment and software advances, meanwhile, have enabled analysis of the outer retinal structure in greater detail. Spectral-domain optical coherence tomography (SD-OCT), for example, is a noninvasive imaging modality providing in vivo images that are comparable to histologic samples, and with good reproducibility as well.[10] SD-OCT also facilitates accuracy, repeatability, and precision in the delineation of individual retinal layers, thereby providing the opportunity for identification of structural biomarkers of varing disease severity.[11]

The outer retina's second hyperreflective band on SD-OCT is a known marker of disease severity in a number of diverse retinal diseases such as age-related macular degeneration (ARMD) and inflammatory disease.[12–15] Whereas traditionally it has been associated with the photoreceptors' inner/outer segment junction, more recent studies suggest an anatomic correlation with the inner segment ellipsoid, which, by international nomenclature consensus, is referred to as the ellipsoid zone (EZ).[16,17] The EZ, as it is densely packed with mitochondria, is essential to photoreceptors' structural integrity and function; indeed, it has important metabolic and light-guiding roles.[18,19] Observation of EZ changes in glaucoma patients, then, has the potential to provide clues to outer retinal involvement in glaucoma.

Hood and associates[20] demonstratred an intensity reduction (albeit associated with a band relatively normal in appearance) of EZ band in patients suffering diminished photoreceptor cone function. Gin and associates[14] suggested, for analysis of EZ band intensity on SD-OCT, a quantitiative

measurement method. Thus prompted, in the present study, we performed an SD-OCT comparative assessment of EZ intensity between glaucoma patients at different disease stages and normal subjects. Our data will provide a starting point for future longitudinal studies seeking to demonstrate an EZ change time course for glaucoma advance.

METHODS

THIS CROSS-SECTIONAL STUDY WAS APPROVED BY THE Seoul National University Hospital Institutional Review Board and faithfully adhered to the tenets of the Declaration of Helsinki.

• **STUDY SUBJECTS:** All of the study subjects were examined between January 1, 2015 and October 31, 2017 at the Seoul National University Hospital Glaucoma Clinic in Seoul, Korea. Based on a retrospective review of medical records, eligible participants were consecutively enrolled. All were subjected to a complete ophthalmic examination, including visual acuity assessment, refraction, slit-lamp biomicroscopy, gonioscopy, Goldmann applanation tonometry (Haag-Streit, Koniz, Switzerland), and dilated stereoscopic examination of the optic disc. Additionally, the subjects underwent the following: central corneal thickness measurement (Orbscan 73 II; Bausch & Lomb Surgical, Rochester, New York, USA), axial length measurement (IOLMaster ver. 5; Carl Zeiss Meditec, Inc, Dublin, California, USA), stereo disc photography (SDP), red-free retinal nerve fiber layer (RNFL) photography, and Cirrus HD-OCT (Carl Zeiss Meditec, Inc), including macular ganglion cell–inner plexiform layer (GCIPL) thickness and central 30-2 threshold testing of the Humphrey Visual Field (HVF) (HFA II; Humphrey Instruments Inc, Dublin, California, USA).

For inclusion in the study, subjects were required to be aged between 40 and 65 years and to have a best-corrected visual acuity greater than or equal to 20/40 in the Snellen equivalent, a spherical refraction greater than −6 diopters (D) and less than 3 D, an open anterior chamber angle, and reliable results on visual field (VF) tests. The exclusion criteria were as follows: (1) a history of intraocular surgery (except cataract surgery) or retinal laser photocoagulation and (2) any neurologic and systemic diseases potentially affecting retinal structure and/or function and VF results. Additionally excluded were any cases of suspicious retinal lesions possibly affecting the outer retinal layer, including inflammatory conditions as well as hereditary and degenerative retinal diseases.

Glaucomatous eyes were defined based on the appearance of the characteristic optic disc (localized or diffuse neuroretinal rim thinning/notching) on SDP and the presence of RNFL defect in the corresponding region on red-free fundus imaging, regardless of the presence or absence of glaucomatous VF defect. Signs of optic disc on SDP and of RNFL on red-free imaging were independently evaluated by 2 glaucoma specialists (A.N.H. and K.H.P.) masked to all other clinical data. Discrepancies between their findings were resolved by consensus. Among the glaucomatous eyes, the preperimetric glaucoma diagnosis was made in cases of a normal VF on conventional HVF. Normal HVF results were defined as mean deviation (MD) and pattern standard deviation within the 95% confidence limits and a glaucoma hemifield test result within the normal limits.

Glaucomatous VF defects were defined as follows: (1) a cluster of 3 points with probabilities less than 5% in at least 1 hemifield on the pattern deviation map, including at least 1 point with a probability less than 1% or a cluster of 2 points with a probability less than 1%; (2) Glaucoma Hemifield Test results outside the normal limits; or (3) a pattern standard deviation beyond 95% of the normal limits, as confirmed by at least 2 reliable examinations (false-positives/negatives $< 15\%$, fixation losses $< 15\%$). Based on a reliable HVF result obtained on the day of SD-OCT imaging, the glaucoma patients were divided into 3 groups: preperimetric glaucoma (no glaucomatous VF defect), mild-to-moderate glaucoma (VF MD ≥ -12 dB), and severe glaucoma (VF MD < -12 dB).

The normal controls had an intraocular pressure (IOP) less than or equal to 21 mm Hg, no history of IOP elevation, no glaucomatous optic disc appearance, no RNFL/GCIPL defect, and normal HVF results. If both eyes were found to be eligible, 1 was selected randomly.

• **IMAGING OF OUTER-RETINAL LAYER:** All of the subjects were scanned by SD-OCT confocal scanning laser ophthalmoscopy (Spectralis HRA+OCT; Heidelberg Engineering, Vista, California, USA) using the eye-tracking feature (TruTrack; Heidelberg Engineering, Heidelberg, Germany). All images were obtained through dilated pupils by a single experienced examiner. Two 9-mm line scans, 1 along the horizontal meridian and the other along the vertical meridian, were obtained with the high-resolution setting, and the images of 128 frames centered on the fovea were averaged. The presence of the foveal bulge, foveal depression, and inner retinal layer thinning, all as seen on SD-OCT, was taken as confirmation of the foveal area. To be included, all images were reviewed for noncentered scans or presence of artifacts, and had a signal quality > 20 dB.

• **ANALYSIS OF ELLIPSOID ZONE:** EZ is known to become less distinct with eccentricity. The mitochondrial packing density in the ellipsoid is lower for rods than for cones, and the proportion of the area occupied by rods increases with eccentricity.[16] Further, the inner segments of the cones become shorter and wider toward the periphery of the retina, resulting in a blurred EZ boundary.[16] In a previous study, EZ remained consistent until about 10 degrees (3000 μm) peripheral from the fovea. Near the 12-degree (3600-μm) periphery, the EZ and interdigitation zone

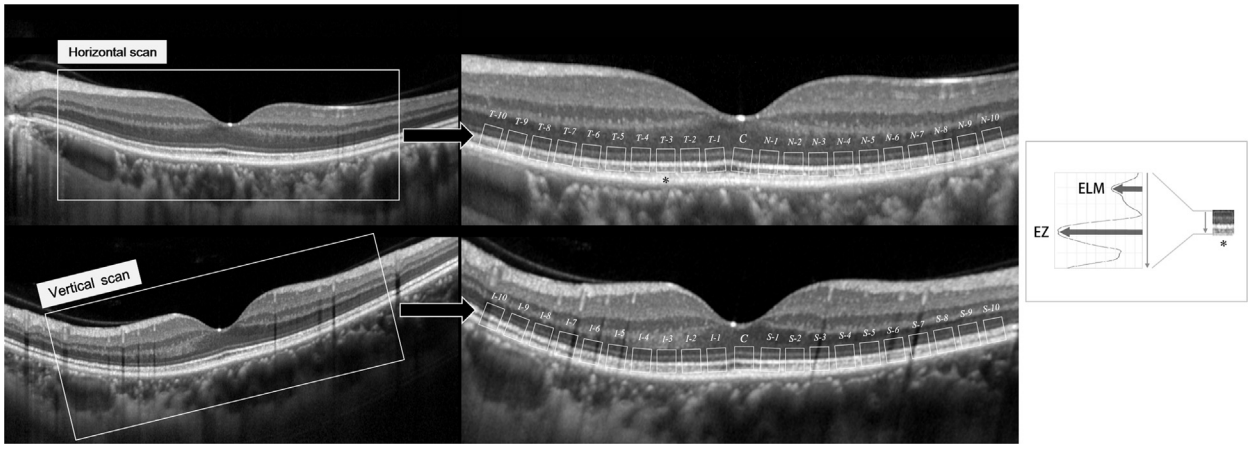

FIGURE 1. Illustrative diagram of 21 retinal locations of ellipsoid zone (EZ) and external limiting membrane (ELM) sampling at fovea and to maximum 2000 μm eccentricity from fovea, both vertically and horizontally. Each sample was 150 μm in width and had 200 μm of interval. Accordingly, the "relative intensity of an EZ segment" was taken as the EZ segment intensity divided by the ELM intensity. Then, the relative EZ intensity was averaged over each retinal segment within the center and 4 sectors: nasal/temporal (Left upper and Middle upper) and superior/inferior (Left lower and Middle lower). (Right) The relative EZ intensity was defined as the highest value of EZ band intensity divided by the highest value of ELM band intensity using the public-domain NIH Image program (ImageJ 1.48v, developed by Wayne Rasband; National Institutes of Health, Bethesda, Maryland, USA). The retinal segment (T-3) used for relative EZ intensity calculation is marked with asterisks.

approached one another and became indistinguishable.[21] Likewise, according to the results of our pilot study on 25 normal and 25 glaucoma eyes, the maximum range in which clear and reliable EZ intensity can be obtained was about 2000 μm from the fovea. In this study, therefore, for the purpose of consistent and accurate EZ intensity measurements, we analyzed only the central macular area (total 4000 μm length). To account for OCT scan brightness variation, the relative EZ intensity was determined as the ratio of the second reflective band to the first (ie, the EZ/external limiting membrane [ELM] ratio). The ELM was used as the anatomic reference for EZ intensity calculation, as it is a nonneural layer maintaining a constant intensity regardless of age or retinal degeneration stage.[16,22] ELM intensity across a wide eccentricity is considered to be relatively constant.[23]

Logarithmic-transformed B-scans (horizontal and vertical SD-OCT line scans through the fovea) for each eye of each participant were analyzed and displayed in tagged image file format (TIFF). The relative EZ intensity in each quadrant (superior, temporal, inferior, nasal) of 4000-μm horizontal and vertical retinal scans through the fovea was averaged, each meridian consisting of 20 retinal segments and one central (C) segment, as shown in Figure 1. Notably, the EZ and ELM were not always parallel to the OCT scan's horizontal plane; thus, for the purpose of consistent and accurate intensity measurements, it was necessary to divide each cross-sectional image into several small segments. Through preliminary validation confirming the optimal number and width of the segments, the method for analyzing an EZ of total 4000 μm length in 150-μm-width segments (resulting in 21 200-μm-interval retinal segments) was determined, and the rectangular segments used for intensity analysis were drawn perpendicularly to the EZ and ELM but not to the OCT horizontal plane.

Relative EZ intensity was measured as the highest EZ band intensity value divided by the highest ELM band intensity value of the SD-OCT images (Figure 1). All of the measurements were performed using the public-domain NIH Image program (ImageJ 1.48v, Wayne Rasband; National Institutes of Health, Bethesda, Maryland, USA). To avoid the local "shadowing" effects of retinal vessels on the EZ and ELM intensity, any segments exhibiting this effect were excluded from further analysis. An experienced ophthalmologist (Y.K.K.) masked to the patients' clinical information performed all of the intensity measurements.

• **STATISTICAL ANALYSIS:** Comparison of the normally distributed demographic data and relative EZ intensities among the 4 groups (ie, normal group and 3 glaucoma [preperimetric, mild-to-moderate, severe] groups) was performed by 1-way analysis of variance with the Tukey post hoc test. The categorical data were analyzed by χ^2 test with Bonferroni correction for multiple comparisons. For comparison of EZ intensity between the affected and unaffected visual hemifield in eyes with glaucoma, the Wilcoxon signed rank test was used. For glaucomatous eyes, Pearson correlation analysis of the relative EZ intensity with average GCIPL or VF MD was performed. In all of the analyses, parametric or nonparametric tests were used

TABLE. Demographic and Baseline Clinical Characteristics of Study Patients

		Glaucoma			
	Normal, N = 37	Preperimetric, N = 38	Mild-to-Moderate, N = 39	Severe, N = 36	*P*
Baseline factors					
Age (y)	57.03 ± 5.38	57.95 ± 6.90	59.10 ± 6.66	59.06 ± 7.00	.469[a]
Male, n (%)	21 (57)	20 (53)	23 (59)	21 (58)	.467[b]
Systemic factors					
Diabetes mellitus, n (%)	4 (11)	4 (11)	5 (13)	4 (11)	.989[b]
Hypertension, n (%)	6 (16)	7 (18)	6 (15)	6 (17)	.987[b]
Cardiovascular disease, n (%)	3 (8)	4 (11)	4 (10)	4 (11)	.976[b]
Ocular factors					
IOP (mm Hg)	12.19 ± 1.61	13.08 ± 1.94	12.03 ± 1.83	12.06 ± 2.41	.140[a]
Central corneal thickness (μm)	533.82 ± 23.12	531.24 ± 29.21	528.31 ± 35.32	524.56 ± 33.97	.609[a]
Spherical equivalent (diopters)	−0.16 ± 1.81	0.00 ± 1.49	−0.36 ± 2.21	−0.32 ± 1.90	.641[a]
Axial length (mm)	24.08 ± 1.40	23.44 ± 1.00	23.78 ± 1.32	23.91 ± 1.13	.145[a]
Lens status, pseudophakic, n (%)	12 (32)	13 (34)	15 (39)	13 (36)	.954[b]
Average GCIPL thickness (μm)	82.82 ± 8.41	78.62 ± 7.31	69.53 ± 4.01	60.93 ± 5.76	<.001[a]
VF MD (dB)	−0.23 ± 0.58	−0.88 ± 0.58	−7.67 ± 1.94	−17.77 ± 3.22	<.001[a]

GCIPL = ganglion cell–inner plexiform layer; IOP = intraocular pressure; VF MD = visual field mean deviation.
Values are shown as mean ± standard deviation unless otherwise indicated.
[a]One-way analysis of variance.
[b]χ^2 test with Bonferroni correction.

based on the normality test, and 95% confidence interval (CI) was calculated. Statistical analysis was performed using the SPSS statistical package (SPSS 22.0; SPSS, Chicago, Illinois, USA), and a *P* value less than .05 was considered statistically significant.

RESULTS

A TOTAL OF 179 EYES (179 SUBJECTS) MEETING THE ENTRY criteria underwent SD-OCT. Twenty-nine eyes (29 subjects) were excluded owing to poor-quality OCT scans. A total of 37 normal eyes (37 subjects), 38 preperimetric glaucomatous eyes (38 subjects), and 75 glaucomatous eyes with VF defect on HVF (75 subjects) were included. All of the enrolled subjects were primary open-angle glaucoma (POAG) patients with untreated IOP ≤ 21 mm Hg (ie, normal-tension glaucoma [NTG] patients). The glaucomatous eyes with VF defect were subdivided as follows: 39 eyes with mild-to-moderate glaucoma (VF MD ≥ −12 dB) and 36 eyes with severe glaucoma (VF MD < −12 dB).

• **DEMOGRAPHIC AND CLINICAL CHARACTERISTICS OF STUDY SUBJECTS:** The demographic characteristics, along with the systemic and ocular factors for each group, are summarized in the Table. The 4 groups' mean age, sex distribution, IOP at time of OCT measurement, central corneal thickness, spherical equivalent, axial length, and lens status were similar ($P = .469$, $P = .467$, $P = .140$, $P = .609$, $P = .641$, $P = .145$, and $P = .954$, respectively). Average GCIPL thickness and VF MD significantly differed across all 4 groups (both $P < .001$).

• **COMPARISON OF RELATIVE ELLIPSOID ZONE INTENSITY BETWEEN NORMAL SUBJECTS AND EYES WITH DIFFERENT STAGES OF GLAUCOMA:** The relative EZ intensity did not show a statistically significant difference between the normal and preperimetric glaucomatous eyes (4.06 ± 0.40, CI 3.92–4.19 vs 3.86 ± 0.44, CI 3.71–4.00, $P = .751$). However, the relative EZ intensities were significantly reduced in glaucomatous eyes with VF defect, both in the mild-to-moderate glaucoma group (3.15 ± 0.43, CI 3.02–3.30, $P < .001$) and in the severe glaucoma group (2.46 ± 0.38, CI 2.33–2.59, $P < .001$), relative to the normal subjects; meanwhile, the relative EZ intensity was much lower in the severe glaucoma group than in the mild-to-moderate glaucoma group ($P < .001$, Figure 2). Figure 3 shows representative OCT scans through the fovea and relative EZ intensities in the normal group and each stage of glaucoma group.

• **RELATIONSHIP OF RELATIVE ELLIPSOID ZONE INTENSITY TO VISUAL FIELD MEAN DEVIATION:** The relative EZ intensity of 75 glaucomatous eyes with VF defect were plotted against their VF MD (Figure 4). The relative EZ intensity and VF MD showed a statistically significant correlation ($r = 0.850$, $P < .001$), and the correlation remained statistically significant after controlling for age ($r = 0.830$, $P < .001$).

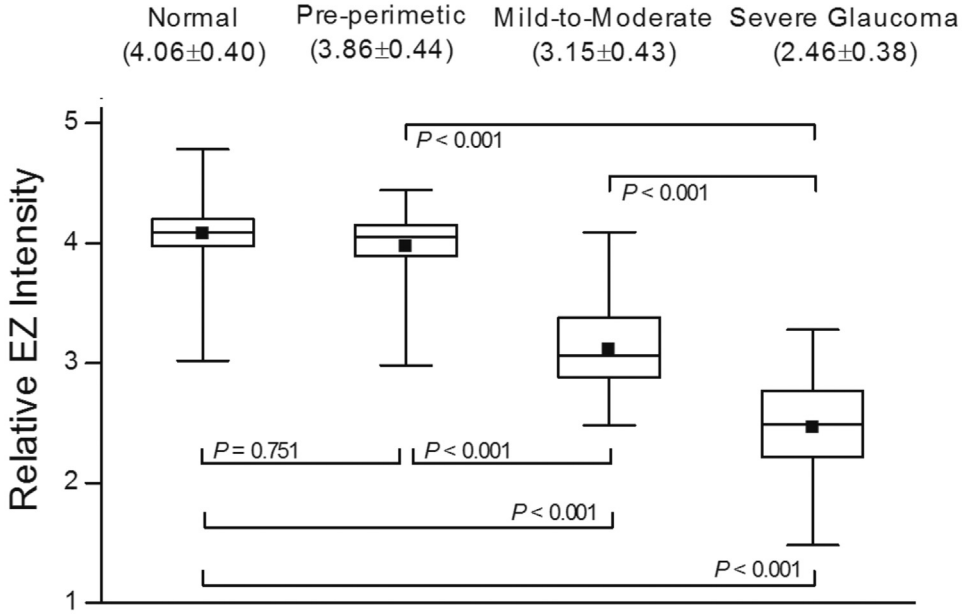

FIGURE 2. Box-and-whisker plot of relative ellipsoid zone (EZ) intensity in each group. The relative EZ intensity was significantly reduced in the mild-to-moderate and severe glaucoma groups ($P < .001$); however, no significant EZ intensity reduction was observed in the preperimetric group relative to the normal group ($P = .751$). Black squares in the box, lines of the ends of the box, and 2 lines outside the box represent the means, upper/lower quartiles, and maximum/minimum values, respectively.

The correlation between relative EZ intensity and VF MD was statistically significant in all 3 glaucoma groups with and without VF defects ($r = 0.357$; $P = .030$, $r = 0.644$; $P < .001$, and $r = 0.732$; $P < .001$, respectively).

• RELATIONSHIP OF RELATIVE ELLIPSOID ZONE INTENSITY TO CENTRAL VISUAL SENSITIVITIES: The relative EZ intensities of 75 glaucomatous eyes with VF defect (ie, the mild-to-moderate and severe glaucoma groups) were plotted against the visual sensitivities of the central 12 points on a pattern deviation map of HVF C30-2 (ie, about 10 degrees of visual angle). The relative EZ intensities and visual sensitivities of the central 12 points showed a statistically significant correlation ($r = 0.557$, $P < .001$), which remained statistically significant after controlling for age ($r = 0.531$, $P < .001$, Figure 4).

• COMPARISON OF RELATIVE ELLIPSOID ZONE INTENSITY ACCORDING TO LOCATION OF PERIMETRIC HEMIFIELD DEFECT: In glaucoma patients showing isolated superior or inferior visual hemifield defect (9 eyes with superior hemifield defect and 12 eyes with inferior hemifield defect), the relative EZ intensities in each hemiretina were compared between the affected and unaffected hemifield (superior VF defect with inferior affected retinal area and inferior VF defect with superior affected retinal area). From the hemifield comparison analysis, segment C was excluded. In the results, the relative EZ intensity (2.98 ± 0.41 vs 3.32 ± 0.39) was significantly reduced in the VF-affected hemiretina ($P = .037$).

• RELATIONSHIP OF RELATIVE ELLIPSOID ZONE INTENSITY TO GANGLION CELL–INNER PLEXIFORM LAYER THICKNESS: The relative EZ intensity and average GCIPL thickness in Cirrus OCT were compared. The relative EZ intensity of 113 glaucomatous eyes with and without VF defect (ie, the preperimetric, mild-to-moderate, and severe glaucoma groups) was plotted against the average GCIPL thickness (Figure 4). The relative EZ intensity and average GCIPL thickness showed a significant correlation ($r = 0.764$, $P < .001$), which remained statistically significant after controlling for age ($r = 0.760$, $P < .001$).

By subgroup analysis, however, in preperimetric and mild-to-moderate glaucoma, the correlation between relative EZ intensity and average GCIPL thickness was not statistically significant ($P = .574$ and $P = .499$, respectively), and the correlation between relative EZ intensity and average GCIPL thickness was statistically significant only in the severe glaucoma group ($r = 0.683$, $P < .001$).

DISCUSSION

HAVING PERFORMED AN IN VIVO EVALUATION OF THE outer retina at different stages of glaucoma, we found that EZ intensity reduction on SD-OCT occurs in the mild-to-moderate and severe glaucoma stages. To our best knowledge, this is the first report to examine EZ intensity change on SD-OCT according to glaucoma stage advancement.

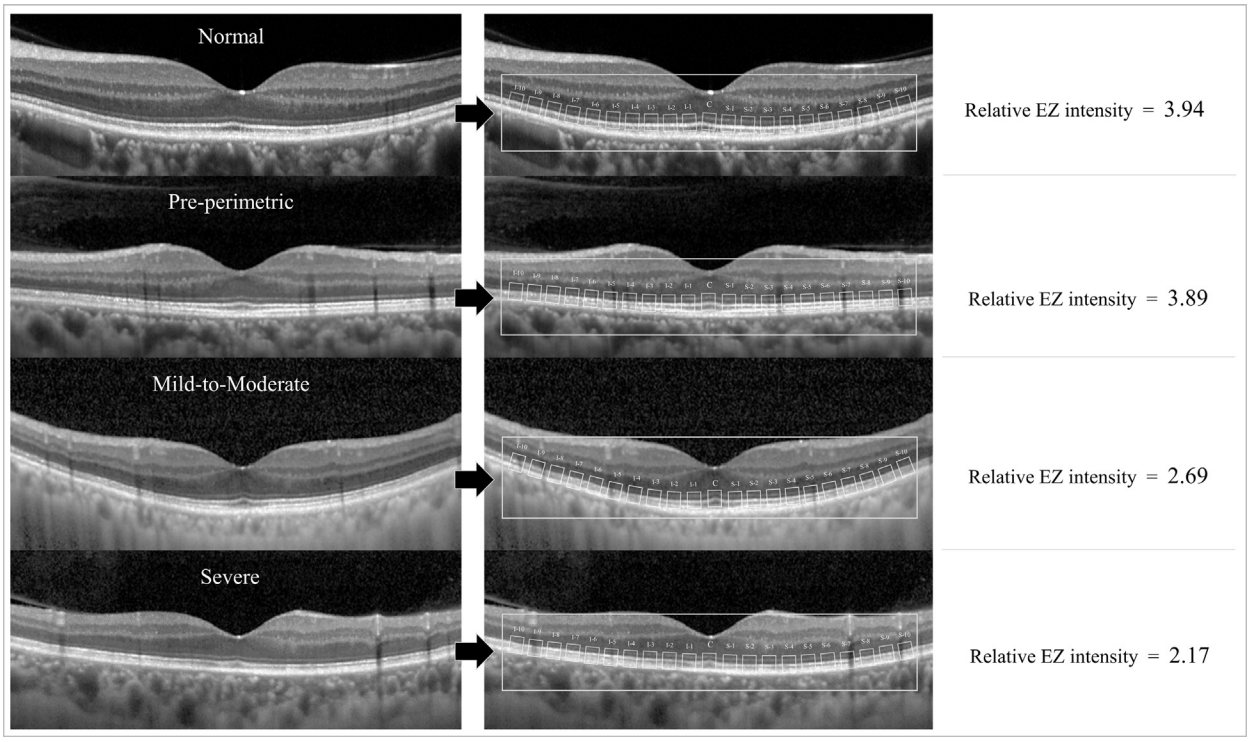

FIGURE 3. Representative high-resolution vertical-line optical coherence tomography scans through fovea and relative ellipsoid zone (EZ) intensities (ie, highest value of EZ band intensity divided by highest value of external limiting membrane intensity) in normal eye (First row) and eyes with different stages of glaucoma: preperimetric (Second row), mild-to-moderate (Third row), and severe (Last row).

The histologic data gathered in the relevant previous studies have suggested that the EZ consistently aligns with the photoreceptors' inner segment ellipsoids, which consist of tightly packed mitochondria.[16] Thus, EZ reflectivity might, at least in part, represent the integrity of mitochondria in photoreceptors.[12] In ARMD, in the pathogenesis of which the mitochondria-related pathways play a key role, EZ band intensity has been found to be significantly lower than in control subjects of a similar age.[15] In another study, reduced EZ intensity was significantly associated with multifocal electroretinogram implicit time delay, indicative of decreased retinal function.[23] In the present study, there was a significant correlation between relative EZ intensity and glaucoma severity: with greater glaucomatous VF damage, EZ intensity was further reduced. On this basis, we may posit that the mitochondria in the inner segments of photoreceptors might be affected in the course of glaucoma progression.

One possible explanation of the EZ intensity reduction mechanism is trans-synaptic degeneration occurring after RGC loss in glaucomatous eyes. Anatomically, RGC dendrites form synapses to the bipolar and amacrine cells, which inter-neurons connect to the photoreceptors.[24] Neurons can affect other synapsed neurons, either directly or indirectly, by retrograde or anterograde degeneration.[25] In the central nervous system, retrograde trans-synaptic degeneration of the optic nerve and ganglion cells has been noted after occipital lesions.[26,27] Embryologic findings supporting the presence of centrifugal (ie, brain-to-retina) fibers along with physiologic evidence of impulses conveyed along those centrifugal fibers have been revealed.[28,29] Gills and associates[30] showed that significant trans-synaptic degeneration also can occur in the inner nuclear layer of the retina following the optic nerve lesions. Progressive retinal thinning consequent upon brain damage owing to stroke in the corresponding region has been demonstrated using SD-OCT ganglion cell layer analysis.[31] Likewise, it has been posited that retrograde trans-synaptic degeneration can take place within the photoreceptors after extensive RGC loss.[32]

There have been conflicting reports on the retrograde trans-synaptic degeneration effect of RGC damage on the outer retina. One of the causes of such inconsistency can be the differing densities of the synapses connected to RGCs and photoreceptors.[24] It is possible that the outer retinal cells are less prone to retrograde trans-synaptic degeneration owing to the fact that they have more collateral neural connections (as has been shown for polyaxonal amacrine cells in the rabbit retina)[33,34] that can guarantee greater supply of neurotrophic factors to the neurons. Additionally, the process of retrograde trans-synaptic degeneration is known to be very slow, especially in more

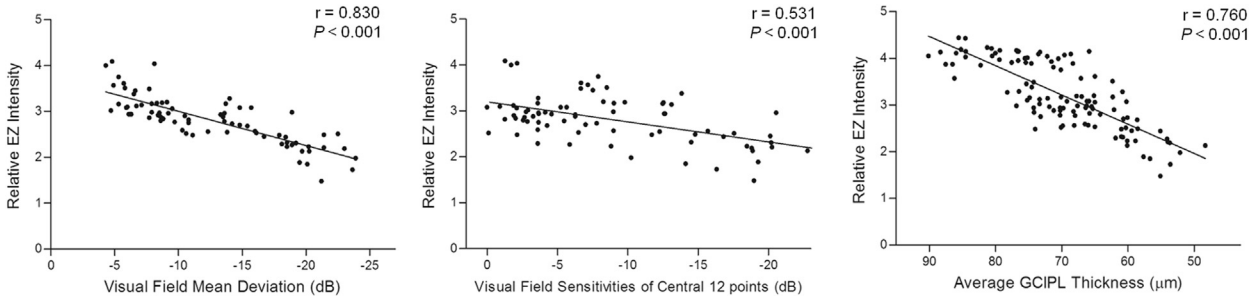

FIGURE 4. Scatterplots of relative ellipsoid zone (EZ) intensity against visual field (VF) mean deviation (MD), visual sensitivities of central 12 points, and average ganglion cell–inner plexiform layer (GCIPL) thickness. In 75 glaucomatous eyes with VF defect (ie, the mild-to-moderate and severe glaucoma groups), the relative EZ intensity showed a statistically significant correlation with VF MD ($r = 0.830$, $P < .001$ after controlling for age, Left) and with the visual sensitivities of the central 12 points on a pattern deviation map of Humphrey Visual Field C30-2 ($r = 0.531$, $P < .001$ after controlling for age, Middle). The relative EZ intensities of 113 glaucomatous eyes with and without VF defect (ie, the preperimetric, mild-to-moderate, and severe glaucoma groups) were plotted against the average GCIPL thickness (Right). A statistically significant correlation ($r = 0.764$, $P < .001$) was shown, which remained statistically significant after controlling for age ($r = 0.760$, $P < .001$).

highly developed animal species,[35] and this might explain the lack of awareness of its clinical significance until now. Furthermore, in most of the previous animal experiments, neurons have been mainly investigated by histology, though metabolic or functional changes can precede actual morphologic alterations to cells, thus masking evidence of retrograde trans-synaptic degeneration in photoreceptors.

Further, RGCs are in close contact with glial cells, of which there are 3 types: Müller cells, astrocytes, and microglia. Under normal conditions, glial cells support neuronal function of photoreceptors via a variety of structural and nutritional mechanisms.[36] At some point, though, a shift in cell function, perhaps triggered by the prolonged stress that is associated with glaucomatous change, seemingly occurs, after which cells are no longer supportive but damaging to neuronal tissue.[37] In such circumstances, glial cells become neurodestructive, thereby releasing increased amounts of neurotoxic substances such as tumor necrosis factor-alpha (TNF-α) and nitric oxide.[25] Generalized loss of astrocyte coverage over the RNFL, and the resultant dysregulation of vascular permeability and endothelial cell activation, have been demonstrated by a rodent experimental model of glaucoma.[38] These alterations in the function of glial cells are expected to cause structural and functional changes in photoreceptor cells. Indeed, based on our results, it can be deduced that advanced glaucoma's discursive damage to RGCs and prolonged stress on glial cells can potentially affect the EZ of the outer retinal layer.

It is known that choroidal hypoperfusion is associated, to some extent, with glaucoma's pathophysiology. Spraul and associates'[39] histologic study found that postmortem eyes manifesting severe glaucomatous damage after long-standing POAG showed a lower-density choriocapillaris at the macula relative to control eyes. By both histologic and angiographic techniques, significantly reduced choroidal thickness, delayed peak choroidal filling, decreased vessel frequency, and smaller mean vessel diameter have been identified in POAG eyes.[40] Given the outer retina's utter dependence on the choriocapillaris for its very high oxygen consumption requirement,[41] lowered choriocapillary blood supply could lead to outer retinal ischemia in advanced stages of POAG, which might, in turn, affect the EZ (ie, mitochondria) in the photoreceptor's inner segments.

According to this study, the relative EZ intensity showed a better correlation with MD of HVF C30-2 than with the visual sensitivities of the central 12 points on the pattern deviation map. It is known that 20-100 cone photoreceptors form synapses with 1 ganglion cell.[42] Considering the effects of surrounding glial cells and choroidal hypoperfusion together, EZ intensity reduction might occur as an overall retinal change during the glaucoma stage advancement rather than focal pathology that directly corresponds to the point of VF defect. That is, glaucomatous damage in the inner retina might be associated with a wider range of the outer retinal change. However, considering the spatial relationship with central macular area, since the HVF C10-2 program tests more points crowded in the macula, further study should be conducted to compare the correlations with EZ intensity among different perimeters.

Interestingly, no EZ intensity reduction was observed in glaucomatous eyes at the preperimetric stage. Werner and associates[43] demonstrated that outer retinal cell loss occurs in cases manifesting long-term visual field loss, on which basis they suggested that outer retinal structural changes lag cell loss in the inner retina. This means that RGC damage exceeding a certain critical point can have a negative effect on photoreceptors. Also, a cell-function shift from neuroprotection to neurodestruction of glial cells has been known to occur only when prolonged stress exceeds a specific point. These results indicate that in early stages of glaucoma at which substantial numbers of RGCs survive, photoreceptor cell functionality might not yet be significantly affected.

Further, in preperimetric and mild-to-moderate glaucoma, EZ intensity showed a significant correlation with VF MD but not with average GCIPL thickness in this study. Especially in the preperimetric group, a decrease in GCIPL thickness was observed, but the relative EZ intensity reduction was not evident. Perhaps, GCIPL thickness reduction precedes the change in EZ intensity, and this suggests that in early-to-moderate-stage glaucoma, a time lag between inner retinal cell loss and outer retinal structural change might exist.

The present study's findings must be interpreted in light of its limitations. First, we defined the ELM as a reference structure, as it does not significantly differ with either age or glaucomatous change.[44] However, we cannot rule out the possibility that subtle ELM intensity changes resulting from undiagnosed pathologies affected our results. Second, artifacts or posterior vitreous detachment can lead to focal intensity change on SD-OCT images. For minimization of this effect, we verified all images manually prior to the intensity analysis in order to identify any conditions possibly affecting the outer retina. Third, intensity was measured within the central 4000 × 4000-μm area, because the ELM and EZ tend to show less clear boundaries toward the periphery on OCT images. Considering the fact that, in glaucoma progression, arcuate defects generally occur first, it is possible that our EZ intensity results would have shown decreases from the earlier disease stage if we had included the intensity values of the more peripheral areas. Further, in order to obtain more accurate and consistent EZ intensity data, the average EZ intensity values of multiple scans within the area of interest should be calculated. Fourth, it is possible that our observation of "no change" in EZ intensity in the early stage of glaucoma was attributable to the current image modality's lack of sufficient sensitivity to detect such change. Fifth, we studied a group of POAG patients with untreated IOP ≤ 21 mm Hg. Our results perhaps might not be directly applicable, therefore, to higher-baseline-IOP POAG patients. Finally, this was a cross-sectional study. A future longitudinal study should be conducted to investigate any correlations of outer retinal layer change with glaucomatous optic neuropathy progression.

In conclusion, relative EZ intensity reduction in the mild-to-moderate and severe glaucoma stages was found on SD-OCT, and the extent of reduction was positively associated with glaucoma severity. These findings tentatively suggest that secondary changes to mitochondria that are packed tightly within photoreceptors' inner segment ellipsoids might occur during glaucoma progression. The clinical significance of potential EZ intensity reduction in glaucoma should be further evaluated.

FUNDING SUPPORT: NO FUNDING OR GRANT SUPPORT. FINANCIAL DISCLOSURES: THE FOLLOWING AUTHORS HAVE NO financial disclosures: Ahnul Ha, Young Kook Kim, Jin Wook Jeoung, and Ki Ho Park. All authors attest that they meet the current ICMJE criteria for authorship.

REFERENCES

1. Quigley HA, Dunkelberger GR, Green WR. Retinal ganglion cell atrophy correlated with automated perimetry in human eyes with glaucoma. *Am J Ophthalmol* 1989;107(5):453–464.
2. Osborne NN, Wood JP, Chidlow G, Bae J-H, Melena J, Nash MS. Ganglion cell death in glaucoma: what do we really know? *Br J Ophthalmol* 1999;83(8):980–986.
3. Yücel YH, Zhang Q, Weinreb RN, Kaufman PL, Gupta N. Effects of retinal ganglion cell loss on magno-, parvo-, koniocellular pathways in the lateral geniculate nucleus and visual cortex in glaucoma. *Prog Retin Eye Res* 2003;22(4):465–481.
4. Panda S, Jonas JB. Decreased photoreceptor count in human eyes with secondary angle-closure glaucoma. *Invest Ophthalmol Vis Sci* 1992;33(8):2532–2536.
5. Nork TM, Ver Hoeve JN, Poulsen GL, et al. Swelling and loss of photoreceptors in chronic human and experimental glaucomas. *Arch Ophthalmol* 2000;118(2):235–245.
6. Velten IM, Korth M, Horn FK. The a-wave of the dark adapted electroretinogram in glaucomas: are photoreceptors affected? *Br J Ophthalmol* 2001;85(4):397–402.
7. Holopigian K, Greenstein VC, Seiple W, Hood DC, Ritch R. Electrophysiologic assessment of photoreceptor function in patients with primary open-angle glaucoma. *J Glaucoma* 2000;9(2):163–168.
8. Kendell KR, Quigley HA, Kerrigan LA, Pease ME, Quigley EN. Primary open-angle glaucoma is not associated with photoreceptor loss. *Invest Ophthalmol Vis Sci* 1995;36(1):200–205.
9. Frishman LJ, Shen FF, Du L, et al. The scotopic electroretinogram of macaque after retinal ganglion cell loss from experimental glaucoma. *Invest Ophthalmol Vis Sci* 1996;37(1):125–141.
10. Ho J, Sull AC, Vuong LN, et al. Assessment of artifacts and reproducibility across spectral-and time-domain optical coherence tomography devices. *Ophthalmology* 2009;116(10):1960–1970.
11. Kiernan DF, Mieler WF, Hariprasad SM. Spectral-domain optical coherence tomography: a comparison of modern high-resolution retinal imaging systems. *Am J Ophthalmol* 2010;149(1):18–31.e12.
12. Tao LW, Wu Z, Guymer RH, Luu CD. Ellipsoid zone on optical coherence tomography: a review. *Clin Exp Ophthalmol* 2016;44(5):422–430.
13. Cai CX, Locke KG, Ramachandran R, Birch DG, Hood DC. A comparison of progressive loss of the ellipsoid zone (EZ) band in autosomal dominant and x-linked retinitis pigmentosa. *Invest Ophthalmol Vis Sci* 2014;55(11):7417–7422.
14. Gin TJ, Wu Z, Chew SK, Guymer RH, Luu CD. Quantitative Analysis of the Ellipsoid Zone Intensity in Phenotypic

Variations of Intermediate Age-Related Macular Degeneration. *Invest Ophthalmol Vis Sci* 2017;58(4):2079–2086.
15. Wu Z, Ayton LN, Guymer RH, Luu CD. Second reflective band intensity in age-related macular degeneration. *Ophthalmology* 2013;120(6):1307–1308.e1.
16. Spaide RF, Curcio CA. Anatomical correlates to the bands seen in the outer retina by optical coherence tomography: literature review and model. *Retina* 2011;31(8):1609.
17. Staurenghi G, Sadda S, Chakravarthy U, Spaide RF. Proposed lexicon for anatomic landmarks in normal posterior segment spectral-domain optical coherence tomography: the IN• OCT consensus. *Ophthalmology* 2014;121(8):1572–1578.
18. Jaiswal M, Haelterman NA, Sandoval H, et al. Impaired mitochondrial energy production causes light-induced photoreceptor degeneration independent of oxidative stress. *PLoS Biol* 2015;13(7):e1002197.
19. Hoang Q, Linsenmeier R, Chung C, Curcio C. Photoreceptor inner segments in monkey and human retina: mitochondrial density, optics, and regional variation. *Vis Neurosci* 2002; 19(4):395–407.
20. Hood DC, Zhang X, Ramachandran R, et al. The inner segment/outer segment border seen on optical coherence tomography is less intense in patients with diminished cone function. *Invest Ophthalmol Vis Sci* 2011;52(13):9703–9709.
21. Jonnal RS, Gorczynska I, Migacz JV, Azimipour M, Zawadzki RJ, Werner JS. The properties of outer retinal band three investigated with adaptive-optics optical coherence tomography. *Invest Ophthalmol Vis Sci* 2017;58: 4559–4568.
22. Sundaram V, Wilde C, Aboshiha J, et al. Retinal structure and function in achromatopsia: implications for gene therapy. *Ophthalmology* 2014;121(1):234–245.
23. Wu Z, Ayton LN, Guymer RH, Luu CD. Relationship between the second reflective band on optical coherence tomography and multifocal electroretinography in age-related macular degeneration. *Invest Ophthalmol Vis Sci* 2013;54(4): 2800–2806.
24. Masland RH. The neuronal organization of the retina. *Neuron* 2012;76(2):266–280.
25. Jindahra P, Petrie A, Plant GT. Retrograde trans-synaptic retinal ganglion cell loss identified by optical coherence tomography. *Brain* 2009;132(3):628–634.
26. Beatty R, Sadun A, Smith L, Vonsattel J, Richardson E. Direct demonstration of transsynaptic degeneration in the human visual system: a comparison of retrograde and anterograde changes. *J Neurol Neurosurg Psychiatry* 1982;45(2): 143–146.
27. Van Buren J. Trans-synaptic retrograde degeneration in the visual system of primates. *J Neurol Neurosurg Psychiatry* 1963;26(5):402.
28. Ohno T. The possibility of centrifugal to the retina in the rat. *Cell Mol Life Sci* 1980;36(12):1400–1401.
29. Wolter JR, Lund O. Reaction of centrifugal nerves in the human retina: two weeks after photocoagulation. *Am J Ophthalmol* 1968;66(2):221–232.
30. Gills JP, Wadsworth JA. Retrograde transsynaptic degeneration of the inner nuclear layer of the retina. *Invest Ophthalmol Vis Sci* 1967;6(4):437–448.
31. Herro AM, Lam BL. Retrograde degeneration of retinal ganglion cells in homonymous hemianopsia. *Clin Ophthalmol* 2015;9:1057.
32. Komáromy AM. The Effect of Ganglion Cell Axotomy on Other Cells in the Porcine Retina [dissertation]. Gainesville: University of Florida; 2002.
33. Famiglietti EV. Polyaxonal amacrine cells of rabbit retina: morphology and stratification of PA1 cells. *J Comp Neurol* 1992;316:391–405.
34. Bleier R. Retrograde transsynaptic cellular degeneration in mammillary and ventral tegmental nuclei following limbic decortication in rabbits of various ages. *Brain Res* 1969; 15(2):365–393.
35. Jindahra P, Petrie A, Plant GT. The time course of retrograde trans-synaptic degeneration following occipital lobe damage in humans. *Brain* 2012;135(Pt 2):534–541.
36. Johnson EC, Morrison JC. Friend or foe? Resolving the impact of glial responses in glaucoma. *J Glaucoma* 2009; 18(5):341.
37. Tezel G. Oxidative stress in glaucomatous neurodegeneration: mechanisms and consequences. *Prog Retin Eye Res* 2006;25(5):490–513.
38. Prasanna G, Hulet C, Desai D, et al. Effect of elevated intraocular pressure on endothelin-1 in a rat model of glaucoma. *Pharmacol Res* 2005;51:41–50.
39. Spraul CW, Lang GE, Lang GK, Grossniklaus HE. Morphometric changes of the choriocapillaris and the choroidal vasculature in eyes with advanced glaucomatous changes. *Vision Res* 2002;42(7):923–932.
40. Yin ZQ, Millar TJ, Beaumont P, Sarks S. Widespread choroidal insufficiency in primary open-angle glaucoma. *J Glaucoma* 1997;6(1):23–32.
41. Kur J, Newman EA, Chan-Ling T. Cellular and physiological mechanisms underlying blood flow regulation in the retina and choroid in health and disease. *Prog Retin Eye Res* 2012; 31(5):377–406.
42. Curcio CA, Allen KA. Topography of ganglion cells in human retina. *J Comp Neurol* 1990;300:5–25.
43. Werner J, Keltner J, Zawadzki R, Choi S. Outer retinal abnormalities associated with inner retinal pathology in nonglaucomatous and glaucomatous optic neuropathies. *Eye* 2011; 25(3):279.
44. Choi SS, Zawadzki RJ, Lim MC, et al. Evidence of outer retinal changes in glaucoma patients as revealed by ultrahigh-resolution in vivo retinal imaging. *Br J Ophthalmol* 2011;95(1):131–141.